

# Millimeter Wave Rotational Spectrum and Centrifugal Distortion of Thioketene, $\text{H}_2\text{C}=\text{C}=\text{S}$

Manfred Winnewisser and Eckhard Schäfer

Physikalisch-Chemisches Institut, Justus-Liebig-Universität Gießen

Z. Naturforsch. **35a**, 483–489(1980); received February 18, 1980

a-type rotational transitions of molecules in the vibrational ground state of thioketene,  $\text{H}_2\text{C}=\text{C}=\text{S}$ , have been measured in the millimeter wavelength region. The measurements yielded improved rotational constants:

$$\begin{aligned}A &= 286\,655(82) \text{ MHz}, \\B &= 5\,659.47596(72) \text{ MHz}, \\C &= 5\,544.51269(72) \text{ MHz}.\end{aligned}$$

A detailed centrifugal distortion analysis by means of Watson's S-reduced Hamiltonian led to the determination of four quartic, two sextic and two higher order distortion constants:

$$\begin{aligned}D_J &= 1.08569(4) \text{ kHz}, & H_{JK} &= 0.716(20) \text{ Hz}, \\D_{JK} &= 168.269(77) \text{ kHz}, & H_{KJ} &= -408.7(73) \text{ Hz}, \\d_1 &= -25.46(68) \text{ Hz}, & L_{KJ} &= 0.65(24) \text{ Hz}, \\d_2 &= -5.21(35) \text{ Hz}, & S_{KJ} &= -0.0533(24) \text{ Hz}.\end{aligned}$$

Effective rotational and centrifugal distortion constants using planarity conditions were calculated. The electric dipole moment of thioketene was determined to be  $\mu = 1.01(3) \text{ D}$ .


## I. Introduction

Intensive studies have been carried out on the rotational spectra of various isotopic species of ketene,  $\text{H}_2\text{C}=\text{C}=\text{O}$ , since 1950 [1–6]. The centrifugal distortion analysis of ketene [3, 4], together with information from additional infrared data [3, 5], enabled Mallinson and Nemes [6] to reevaluate the molecular force field for ketene. Recently, microwave investigations on the higher homologues thioketene,  $\text{H}_2\text{C}=\text{C}=\text{S}$  [7, 8], and selenoketene,  $\text{H}_2\text{C}=\text{C}=\text{Se}$  [9, 10], have been reported.

The first interstellar microwave detection of interstellar ketene was reported in 1977 by Turner [11]. The detection in the source Sgr B2 was based on three transitions:  $5_{14}-4_{13}$ ,  $5_{15}-4_{14}$  and  $4_{13}-3_{12}$  at the frequencies 101 981.39, 100 094.51 and 81 586.19 MHz, respectively. Further millimeter wave transitions were tentatively detected and assigned. Recently, Thaddeus and coworkers have identified isothiocyanic acid, HNCS [12], and methyl mercaptan,  $\text{CH}_3\text{SH}$  [13], in Sgr B2 from observations of a number of millimeter wave

rotational transitions. The abundances of both of these sulfur-containing molecules, relative to their oxygen analogues which had previously been detected in interstellar dust clouds, imply a sulfur/oxygen ratio not very different from the terrestrial value. Therefore, the detection of the five-atomic molecule  $\text{H}_2\text{C}=\text{C}=\text{S}$  in interstellar dust clouds might become possible with more sensitive instrumentation. The predicted rotational transition frequencies based on the measured millimeter wave spectrum, together with calculated standard deviations, provide the basis for a possible search for interstellar thioketene.

Moreover, thioketene has raised some interest due to the fact that it is a more stable isomer of thiirene,  $\text{H}-\text{C}=\text{C}-\text{H}$ , according to SCF-calculations [14,

15]. These calculations also reveal the fact that ethynylmercaptane,  $\text{H}-\text{C}\equiv\text{C}-\text{SH}$ , should have the same stability as thioketene. As a matter of fact, Krantz and Laurenzi [16] detected both ethynylmercaptane and thioketene in the photolysis of 1,2,3-thiadiazole. However, no ethynylmercaptane was found in the products of pyrolysis reactions [14]. This was confirmed by our microwave experiments.

Reprint requests to Manfred Winnewisser, Physikalisch-Chemisches Institut, Justus-Liebig-Universität Gießen, Heinrich-Buff-Ring 58, D-6300 Gießen.

0340-4811 / 80 / 0500-0483 \$ 01.00/0. — Please order a reprint rather than making your own copy.



Dieses Werk wurde im Jahr 2013 vom Verlag Zeitschrift für Naturforschung in Zusammenarbeit mit der Max-Planck-Gesellschaft zur Förderung der Wissenschaften e.V. digitalisiert und unter folgender Lizenz veröffentlicht: Creative Commons Namensnennung-Keine Bearbeitung 3.0 Deutschland Lizenz.

Zum 01.01.2015 ist eine Anpassung der Lizenzbedingungen (Entfall der Creative Commons Lizenzbedingung „Keine Bearbeitung“) beabsichtigt, um eine Nachnutzung auch im Rahmen zukünftiger wissenschaftlicher Nutzungsformen zu ermöglichen.

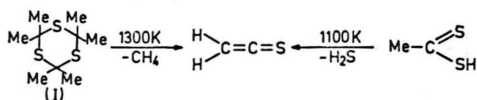
This work has been digitalized and published in 2013 by Verlag Zeitschrift für Naturforschung in cooperation with the Max Planck Society for the Advancement of Science under a Creative Commons Attribution-NoDerivs 3.0 Germany License.

On 01.01.2015 it is planned to change the License Conditions (the removal of the Creative Commons License condition “no derivative works”). This is to allow reuse in the area of future scientific usage.



## II. Experimental Procedures

Thioketene was produced in two different ways (Scheme I).



Scheme I.

As in the report on the earlier microwave measurements of thioketene [8], hexamethyltrithiane (I) was pyrolysed at 1300 K to give thioketene, which was directly pumped through the 2 m glass cell of the millimeter wave spectrometer as shown in Figure 1. Infrared analysis of the gas mixture after pyrolysis showed that a large fraction of the products consisted of ethylene, propylene and allene, thus indicating that only a rather poor yield of thioketene is obtainable by this method. A recently reported procedure [14] of preparing thioketene by pyrolysing dithioacetic acid (Scheme I) was found to yield a considerably higher intensity of the absorption lines, thus indicating higher column densities of  $\text{H}_2\text{CCS}$ .

Attempts to isolate thioketene have failed so far. It could be trapped (spectrum disappears) at temperatures below about 150 K, but polymerised upon warming. Even in the gas phase, at sample pressures of 40  $\mu\text{bar}$ , decay took place with a half-life of about five minutes, independent of the way of preparation. The use of argon as carrier gas in order to entrain the thioketene did not improve the stability.

Microwave measurements were performed near 22 GHz in order to determine the dipole moment using a Hewlett-Packard spectrometer, model 8460 MRR. The millimeter-wave measurements were carried out with a spectrometer described by Winnewisser et al. [19, 20]. A block diagram of the newly improved version of the spectrometer is shown in Fig. 1 and a detailed description of recent improvements is given by Helms et al. [21]. The microwave power was generated by reflex klystrons in the range from 28–40 GHz and multiplied by means of harmonic generation. The multiplier diodes used were phosphorus diffused p-type Si/W point contact diodes and were prepared and mounted in our laboratory using a slightly simplified variant of the method of Burrus [22, 17]. Used together with a recently installed liquid helium cooled InSb detector

[21] they proved to generate sufficient power for measuring transitions up to 475 GHz. All measurements were carried out with the help of a digital data acquisition system [20] to improve the signal-to-noise ratio and to measure automatically the transition frequencies. The accuracy of the measurements is better than 20 kHz at a klystron fundamental frequency of 40 GHz. Sample pressure in the cell was in the range 20–60  $\mu\text{bar}$ .

## III. Assignment of the Measured Rotational Transitions

The available data on thioketene from the earlier measurements [7] enabled us to predict the entire ground-state rotational spectrum in the millimeter wave region with some certainty. The most intense absorption lines in the observed frequency range could easily be assigned to thioketene ground state transitions. The spectrum shows the characteristic pattern of a-type  $^9\text{R}$ -branch rotational transitions. It differs only slightly from the ketene spectrum, having slightly less inertial asymmetry:

$$\alpha(\text{CH}_2\text{CCS}) = -0.99918, \quad \alpha(\text{H}_2\text{CCO}) = -0.99722.$$

Figure 2 shows an oscilloscope display of the most intense lines of the  $J = 10 \leftarrow 9$  transition together with the assignment of the ground state spectrum. The splitting of the  $K_a = 1$  lines is 1.15 GHz, which places them outside the represented frequency range. Their intensity is comparable to the  $K_a = 5$  line intensity. The intensities of the transitions follow basically an asymmetric top intensity distribution modulated by the spin statistics due to the two protons; because of the molecular  $\text{C}_{2v}$  symmetry, transitions arising from odd  $K_a$  levels have three times the statistical weight of those arising from even  $K_a$  levels. Ground state transitions with  $K_a > 7$  have intensities comparable to excited vibrational state transitions. Therefore the measurement and assignment of these weaker lines require precise predictions, which however could not be provided by the centrifugal distortion analysis (see discussion).

Table 1 gives the line frequencies of the observed and calculated transitions. It was impossible to resolve  $K_a$  doublets for  $K_a > 2$ .  $K_a > 3$  and  $K_a = 3$ ,  $J > 11$  line frequencies were assigned and fitted to just one of the doublet transitions. For  $J > 10$  the observed  $K_a = 3$  lines were fitted to both components which were weighted equally. For  $J > 17$  these lines

TABLE 1. Ground State Rotational Transitions of Thickness of the  $\alpha$ -Type B-Ranch.

Transition $J (K_u, K_v) \rightarrow J (K_u, K_v)$	Frequency / MHz		obs.-calc. / MHz	$\nu_{upper}$ / cm <sup>-1</sup>
	observed	calculated (Standard Deviation)		
1 (0, 1) $\rightarrow$ 0 (0, 0)	11201.9842(5)		0.000	0.374
2 (0, 2) $\rightarrow$ 1 (0, 1)	22407.8021(10)		- 0.3	0.753
2 (1, 1) $\rightarrow$ 1 (1, 0)	22522.222		- 6.3	9.753
2 (2, 2) $\rightarrow$ 1 (2, 1)	22592.3054(7)		- 9.6	9.750
3 (0, 3) $\rightarrow$ 2 (0, 2)	33611.7076(16)		- 7.6	3.123
3 (1, 2) $\rightarrow$ 2 (1, 1)	33638.2761(24)		- 2.5	10.493
3 (2, 3) $\rightarrow$ 2 (2, 2)	33783.127 <sup>a</sup>		- 74.8	10.495
3 (3, 4) $\rightarrow$ 2 (3, 3)	33807.9136(11)		- 71.6	38.423
4 (0, 4) $\rightarrow$ 3 (0, 3)	44815.3239(19)		2.482	11.469
4 (1, 3) $\rightarrow$ 3 (1, 2)	44834.3368(32)		11.632	39.744
4 (2, 4) $\rightarrow$ 3 (2, 3)	44810.1281(14)		39.744	86.586
4 (3, 5) $\rightarrow$ 3 (3, 4)	44802.3621(15)		3.727	33.096
5 (0, 5) $\rightarrow$ 4 (0, 4)	55730.1642(28)		13.096	41.239
5 (1, 4) $\rightarrow$ 4 (1, 3)	56304.9549(36)		86.586	103.932
5 (2, 5) $\rightarrow$ 4 (2, 4)	56012.6291(17)		33.124	15.006
5 (3, 6) $\rightarrow$ 4 (3, 5)	56013.2297(17)		41.239	15.006
5 (4, 7) $\rightarrow$ 4 (4, 6)	56004.0415(18)		103.932	5.8
6 (0, 6) $\rightarrow$ 5 (0, 5)	67221.7649		15.006	16.006
6 (1, 5) $\rightarrow$ 5 (1, 4)	67215.8291(46)		16.006	35.012
6 (2, 6) $\rightarrow$ 5 (2, 5)	67165.5556(41)		3.6	42.107
6 (3, 7) $\rightarrow$ 5 (3, 6)	67115.9137(20)		-23.9	89.848
6 (4, 8) $\rightarrow$ 5 (4, 7)	67094.4624		-16.4	105.468
6 (5, 9) $\rightarrow$ 5 (5, 8)	67189.4865(21)		16.2	238.077
6 (6, 10) $\rightarrow$ 5 (6, 9)	67189.1792(22)		10.6	7.848
7 (0, 7) $\rightarrow$ 6 (0, 6)	78424.4554(49)		16.006	17.385
7 (1, 6) $\rightarrow$ 6 (1, 5)	78021.2731(49)		37.385	17.384
7 (2, 7) $\rightarrow$ 6 (2, 6)	78025.9431(46)		46.349	45.349
7 (3, 8) $\rightarrow$ 6 (3, 7)	78016.4538(22)		78418.4332(12)	19.788
7 (4, 9) $\rightarrow$ 6 (4, 8)	78005.0585(24)		- 5.4	47.965
7 (5, 10) $\rightarrow$ 6 (5, 9)	78007.3788(24)		157.701	241.817
7 (6, 11) $\rightarrow$ 6 (6, 10)	78003.4761(25)		344.453	30.444
8 (0, 8) $\rightarrow$ 7 (0, 7)	89624.2225(12)		10.444	19.788
8 (1, 7) $\rightarrow$ 7 (1, 6)	89146.4371(22)		19.788	47.965
8 (2, 8) $\rightarrow$ 7 (2, 7)	89064.0825(49)		47.965	89.848
8 (3, 9) $\rightarrow$ 7 (3, 8)	89021.3378(24)		89.848	160.316
8 (4, 10) $\rightarrow$ 7 (4, 9)	89005.3474(49)		160.316	244.431
8 (5, 11) $\rightarrow$ 7 (5, 10)	89168.0095(13)		347.044	448.117
8 (6, 12) $\rightarrow$ 7 (6, 11)	89176.0938(13)		33.464	13.464
9 (0, 9) $\rightarrow$ 8 (0, 8)	100818.5016		- 2.7	22.782
9 (1, 8) $\rightarrow$ 8 (1, 7)	100311.4186(54)		- 10.5	22.780
9 (2, 9) $\rightarrow$ 8 (2, 8)	100345.5216		- 3.1	50.954
9 (3, 10) $\rightarrow$ 8 (3, 9)	100819.9893		- 11.1	97.794
9 (4, 11) $\rightarrow$ 8 (4, 10)	100824.0884(25)		10.0	163.304
9 (5, 12) $\rightarrow$ 8 (5, 11)	100805.4270		6.1	247.419
10 (0, 10) $\rightarrow$ 9 (0, 9)	107922.4540		9.9	287.419
10 (1, 9) $\rightarrow$ 9 (1, 8)	107937.1378(26)			

<sup>a</sup> Not used in the fit because of overfitting or unresolvable E-to-basis.

TABLE 2 continued

Transition $J (K_u, K_v) \rightarrow J (K_u, K_v)$	Frequency / MHz		obs.-calc. / MHz	$\nu_{upper}$ / cm <sup>-1</sup>
	observed	calculated (Standard Deviation)		
9 (6, 4) $\rightarrow$ 8 (6, 3)	100712.2599	100712.2485(43)	11.4	350.52
9 (7, 5) $\rightarrow$ 8 (7, 4)	100659.9786	100659.9807(54)	- 2.1	471.102
10 (0, 10) $\rightarrow$ 9 (0, 9)	112029.7054	112029.7246(34)	- 16.8	16.817
10 (1, 9) $\rightarrow$ 9 (1, 8)	111656.0481	111656.0496(55)	- 1.4	74.168
10 (2, 10) $\rightarrow$ 9 (2, 9)	112005.4688	112005.4732(63)	- 4.4	74.201
10 (3, 11) $\rightarrow$ 9 (3, 10)	112021.0942	112021.0984(74)	- 5.6	84.317
10 (4, 12) $\rightarrow$ 9 (4, 11)	112026.8519	112026.8604(27)	- 16.5	54.218
10 (5, 13) $\rightarrow$ 9 (5, 12)	112005.3949	112005.3972(100)	2.2	101.157
10 (6, 14) $\rightarrow$ 9 (6, 13)	111979.9963	111979.9963	18.6	161.456
10 (7, 15) $\rightarrow$ 9 (7, 14)	111946.0001	111946.0046(38)	- 5.5	250.779
10 (8, 16) $\rightarrow$ 9 (8, 15)	111901.7216	111901.7245(45)	- 2.9	353.432
10 (9, 17) $\rightarrow$ 9 (9, 16)	111843.8209	111843.8474(57)	- 74.7	474.459
11 (0, 11) $\rightarrow$ 10 (0, 10)	122210.3252	122210.3351(24)	- 9.5	70.554
11 (1, 10) $\rightarrow$ 10 (1, 9)	122006.3326	122006.3326	- 5.0	79.826
11 (2, 11) $\rightarrow$ 10 (2, 10)	122064.6482	122064.6536(53)	- 5.3	30.034
11 (3, 12) $\rightarrow$ 10 (3, 11)	122221.9645	122221.9762(28)	- 7.7	58.054
11 (4, 13) $\rightarrow$ 10 (4, 12)	122090.9590	122090.9652(47)	- 22.0	58.054
11 (5, 14) $\rightarrow$ 10 (5, 13)	122029.6510	122029.6697(68)	- 11.8	474.190
11 (6, 15) $\rightarrow$ 10 (6, 14)	122006.1045	122006.1079(13)	- 3.6	104.893
11 (7, 16) $\rightarrow$ 10 (7, 15)	122005.1112(31)	122005.1112(31)	3.2	170.401
11 (8, 17) $\rightarrow$ 10 (8, 16)	122137.0763	122137.0763	18.4	254.513
11 (9, 18) $\rightarrow$ 10 (9, 17)	122139.7462	122139.7462	- 3.2	357.144
12 (0, 12) $\rightarrow$ 11 (0, 11)	134030.2741	134030.2741	3.0	24.464
12 (1, 11) $\rightarrow$ 11 (1, 10)	133744.2628	133744.2628	33.9	33.916
12 (2, 12) $\rightarrow$ 11 (2, 11)	133523.4397	133523.4428(52)	- 3.2	34.839
12 (3, 13) $\rightarrow$ 11 (3, 12)	134022.5134	134022.5134	6.0	42.164
12 (4, 14) $\rightarrow$ 11 (4, 13)	134040.5764	134040.5764	6.6	169.003
12 (5, 15) $\rightarrow$ 11 (5, 14)	134037.9425	134037.9425	- 12.6	169.003
12 (6, 16) $\rightarrow$ 11 (6, 15)	134033.1943(43)	134033.1943(43)	31.7	174.510
12 (7, 17) $\rightarrow$ 11 (7, 16)	134278.9225	134278.9225	3.5	361.750
12 (8, 18) $\rightarrow$ 11 (8, 17)	134210.2101	134210.2224(57)	- 12.3	482.294
12 (9, 19) $\rightarrow$ 11 (9, 18)	134029.4681	134029.4681	- 5.8	29.145
12 (10, 20) $\rightarrow$ 11 (10, 19)	134087.2576	134087.2576	7.0	38.277
12 (11, 21) $\rightarrow$ 11 (11, 20)	134031.8057(50)	134031.8057(50)	- 6.5	38.676
12 (12, 22) $\rightarrow$ 11 (12, 21)	134022.6678	134022.6678	- 2.3	66.648
12 (13, 23) $\rightarrow$ 11 (13, 22)	134025.4592	134025.4592	42.7	66.649
12 (14, 24) $\rightarrow$ 11 (14, 23)	134020.8221	134020.8221	33.4	112.486
12 (15, 25) $\rightarrow$ 11 (15, 24)	134002.4095(32)	134002.4095(32)	12.6	112.486
12 (16, 26) $\rightarrow$ 11 (16, 25)	134057.4271(32)	134057.4271(32)	- 28.8	78.992
12 (17, 27) $\rightarrow$ 11 (17, 26)	134052.2389	134052.2389	- 19.6	262.102
12 (18, 28) $\rightarrow$ 11 (18, 27)	134046.5761	134046.5761	- 12.5	365.778
12 (19, 29) $\rightarrow$ 11 (19, 28)	134039.0812(58)	134039.0812(58)	14.9	466.771
13 (0, 13) $\rightarrow$ 12 (0, 12)	154627.4757	154627.4757	- 3.1	34.008
13 (1, 12) $\rightarrow$ 12 (1, 11)	154630.8084(48)	154630.8084(48)	- 9.2	43.210
13 (2, 13) $\rightarrow$ 12 (2, 12)	154639.7466	154639.7466	- 40.3	43.559
13 (3, 14) $\rightarrow$ 12 (3, 13)	154622.4152	154622.4152	- 1.3	71.505
13 (4, 15) $\rightarrow$ 12 (4, 14)	154608.2632	154608.2632	- 3.6	71.507
13 (5, 16) $\rightarrow$ 12 (5, 15)	154602.7331	154602.7331	10.2	118.340
13 (6, 17) $\rightarrow$ 12 (6, 16)	154606.7028	154606.7028	- 15.0	180.840
13 (7, 18) $\rightarrow$ 12 (7, 17)	154619.0765	154619.0765	- 6.8	267.956
13 (8, 19) $\rightarrow$ 12 (8, 18)	154656.9347	154656.9347	- 5.9	370.582
13 (9, 20) $\rightarrow$ 12 (9, 19)	154675.6345	154675.6345	12.7	491.621
13 (10, 21) $\rightarrow$ 12 (10, 20)	154602.4584(40)	154602.4584(40)	- 41.8	39.237
13 (11, 22) $\rightarrow$ 12 (11, 21)	154673.4160	154673.4160	- 28.8	48.414
13 (12, 23) $\rightarrow$ 12 (12, 22)	154697.1089(47)	154697.1089(47)	- 28.7	48.817
13 (13, 24) $\rightarrow$ 12 (13, 23)	154602.7032	154602.7032	- 18.1	76.736

TABLE 3 continued

Transition $J (K_u, K_v) \rightarrow J (K_u, K_v)$	Frequency / MHz		obs.-calc. / MHz	$\nu_{upper}$ / cm <sup>-1</sup>
	observed	calculated (Standard Deviation)		
15 (2, 13) $\rightarrow$ 14 (2, 12)	184041.3243	184041.3202(42)	4.1	76.738
15 (3, 14) $\rightarrow$ 14 (3, 13)	184001.3817	184001.3538(55)	- 28.1	123.573
15 (4, 15) $\rightarrow$ 14 (4, 14)	184001.3817	184001.3843(55)	- 12.4	123.573
15 (5, 16) $\rightarrow$ 14 (5, 15)	183982.4387	183982.4427(54)	- 3.7	189.077
15 (6, 17) $\rightarrow$ 14 (6, 16)	183911.5307	183911.5307(45)	- 800.2	273.164
15 (7, 18) $\rightarrow$ 14 (7, 17)	183844.9545	183844.9545(45)	6.5	375.807
15 (8, 19) $\rightarrow$ 14 (8, 18)	183757.7828	183757.8186(55)	- 27.0	496.045
15 (9, 20) $\rightarrow$ 14 (9, 19)	179222.0445	179222.0546(46)	- 9.5	44.462
15 (10, 21) $\rightarrow$ 14 (10, 20)	180135.4500	180135.4587(46)	- 7.2	53.931
15 (11, 22) $\rightarrow$ 14 (11, 21)	180151.9701	180151.9707(46)	- 7.6	84.451
15 (12, 23) $\rightarrow$ 14 (12, 22)	179720.5399	179720.5386(56)	- 6.7	82.341
15 (13, 24) $\rightarrow$ 14 (13, 23)	179359.6541	179359.6599(57)	34.2	129.127
15 (14, 25) $\rightarrow$ 14 (14, 24)	179359.6541	179359.7162(57)	- 22.8	129.127
15 (15, 26) $\rightarrow$ 14 (15, 25)	179359.6541	179359.7162(57)	- 22.8	129.127
15 (16, 27) $\rightarrow$ 14 (16, 26)	179359.6541	179359.7162(57)	- 22.8	129.127
15 (17, 28) $\rightarrow$ 14 (17, 27)	179359.6541	179359.7162(57)	- 22.8	129.127
15 (18, 29) $\rightarrow$ 14 (18, 28)	179359.6541	179359.7162(57)	- 22.8	129.127
15 (19, 30) $\rightarrow$ 14 (19, 29)	179359.6541	179359.7162(57)	- 22.8	129.127
15 (20, 31) $\rightarrow$ 14 (20, 30)	179359.6541	179359.7162(57)	- 22.8	129.127
15 (21, 32) $\rightarrow$ 14 (21, 31)	179359.6541	179359.7162(57)	- 22.8	129.127
15 (22, 33) $\rightarrow$ 14 (22, 32)	179359.6541	179359.7162(57)	- 22.8	129.127
15 (23, 34) $\rightarrow$ 14 (23, 33)	179359.6541	179359.7162(57)	- 22.8	129.127
15 (24, 35) $\rightarrow$ 14 (24, 34)	179359.6541	179359.7162(57)	- 22.8	129.127
15 (25, 36) $\rightarrow$ 14 (25, 35)	179359.6541	179359.7162(57)	- 22.8	129.127
15 (26, 37) $\rightarrow$ 14 (26, 36)	179359.6541	179359.7162(57)	- 22.8	129.127
15 (27, 38) $\rightarrow$ 14 (27, 37)	179359.6541	179359.7162(57)	- 22.8	129.127
15 (28, 39) $\rightarrow$ 14 (28, 38)	179359.6541	179359.7162(57)	- 22.8	129.127
15 (29, 40) $\rightarrow$ 14 (29, 39)	179359.6541	179359.7162(57)	- 22.8	129.127
15 (30, 41) $\rightarrow$ 14 (30, 40)	179359.6541	179359.7162(57)	- 22.8	129.127
15 (31, 42) $\rightarrow$ 14 (31, 41)	179359.6541	179359.7162(57)	- 22.8	129.127
15 (32, 43) $\rightarrow$ 14 (32, 42)	179359.6541	179359.7162(57)	- 22.8	129.127
15 (33, 44) $\rightarrow$ 14 (33, 43)	179359.6541	179359.7162(57)	- 22.8	129.127
15 (34, 45) $\rightarrow$ 14 (34, 44)	179359.6541	179359.7162(57)	- 22.8	129.127
15 (35, 46) $\rightarrow$ 14 (35, 45)	179359.6541	179359.7162(57)	- 22.8	129.127
15 (36, 47) $\rightarrow$ 14 (36, 46)	179359.6541	179359.7162(57)	- 22.8	129.127
15 (37, 48) $\rightarrow$ 14 (37, 47)	179359.6541	179359.7162(57)	- 22.8	129.127
15 (38, 49) $\rightarrow$ 14 (38, 48)	179359.6541	179359.7162(57)	- 22.8	129.127
15 (39, 50) $\rightarrow$ 14 (39, 49)	179359.6541	179359.7162(57)	- 22.8	129.127
15 (40, 51) $\rightarrow$ 14 (40, 50)	179359.6541	179359.7162(57)	- 22.8	129.127
15 (41, 52) $\rightarrow$ 14 (41, 51)	179359.6541	179359.7162(57)	- 22.8	129.127
15 (42, 53) $\rightarrow$ 14 (42, 52)	179359.6541	179359.7162(57)	- 22.8	129.127
15 (43, 54) $\rightarrow$ 14 (43, 53)	179359.6541	179359.7162(57)	- 22.8	129.127
15 (44, 55) $\rightarrow$ 14 (44, 54)	179359.6541	179359.7162(57)	- 22.8	129.127
15 (45, 56) $\rightarrow$ 14 (45, 55)	179359.6541	179359.7162(57)	- 22.8	129.127
15 (46, 57) $\rightarrow$ 14 (46, 56)	179359.6541	179359.7162(57)	- 22.8	129.127
15 (47, 58) $\rightarrow$ 14 (47, 57)	179359.6541	179359.7162(57)	- 22.8	129.127
15 (48, 59) $\rightarrow$ 14 (48, 58)	179359.6541	179359.7162(57)	- 22.8	129.127
15 (49, 60) $\rightarrow$ 14 (49, 59)	179359.6541	179359.7162(57)	- 22.8	129.127
15 (50, 61) $\rightarrow$ 14 (50, 60)	179359.6541	179359.7162(57)	- 22.8	129.127
15 (51, 62) $\rightarrow$ 14 (51, 61)	179359.6541	179359.7162(57)	- 22.8	129.127
15 (52, 63) $\rightarrow$ 14 (52, 62)	179359.6541	179359.7162(57)	- 22.8	129.127
15 (53, 64) $\rightarrow$ 14 (53, 63)	179359.6541	179359.7162(57)	- 22.8	129.127
15 (54, 65) $\rightarrow$ 14 (54, 64)	179359.6541	179359.7162(57)	- 22.8	129.127
15 (55, 66) $\rightarrow$ 14 (55, 65)	179359.6541	179359.7162(57)	- 22.8	129.127
15 (56, 67) $\rightarrow$ 14 (56, 66)	179359.6541	179359.7162(57)	- 22.8	129.127
15 (57, 68) $\rightarrow$ 14 (57, 67)	179359.6541	179359.7162(57)	- 22.8	129.127
15 (58, 69) $\rightarrow$ 14 (58, 68)	179359.6541	179359.7162(57)	- 22.8	129.127
15 (59, 70) $\rightarrow$ 14 (59, 69)	179359.6541	179359.7162(57)	- 22.8	129.127
15 (60, 71) $\rightarrow$ 14 (60, 70)	179359.6541	179359.7162(57)	- 22.8	129.127
15 (61, 72) $\rightarrow$ 14 (61, 71)	179359.6541	179359.7162(57)	- 22.8	129.127
15 (62, 73) $\rightarrow$ 14 (62, 72)	179359.6541	179359.7162(57)	- 22.8	129.127
15 (63, 74) $\rightarrow$ 14 (63, 73)	179359.6541	179359.7162(57)	- 22.8	129.127
15 (64, 75) $\rightarrow$ 14 (64, 74)	179359.6541	179359.7162(57)	- 22.8	129.127
15 (65, 76) $\rightarrow$ 14 (65, 75)	179359.6541	179359.7162(57)	- 22.8	129.127
15 (66, 77) $\rightarrow$ 14 (66, 76)	179359.6541	179359.7162(57)	- 22.8	129.127
15 (67, 78) $\rightarrow$ 14 (67, 77)	179359.6541	179359.7162(57)	- 22.8	129.127
15 (68, 79) $\rightarrow$ 14 (68, 78)	179359.6541	179359.7162(57)	- 22.8	129.127
15 (69, 80) $\rightarrow$ 14 (69, 79)	179359.6541	179359.7162(57)	- 22.8	129.127
15 (70, 81) $\rightarrow$ 14 (70, 80)	179359.6541	179359.7162(57)	- 22.8	129.127
15 (71, 82) $\rightarrow$ 14 (71, 81)	179359.6541	179359.7162(57)	- 22.8	129.127
15 (72, 83) $\rightarrow$ 14 (72, 82)	179359.6541	179359.7162(57)	- 22.8	129.127
15 (73, 84) $\rightarrow$ 14 (73, 83)	179359.6541	179359.7162(57)	- 22.8	129.127
15 (74, 85) $\rightarrow$ 14 (74, 84)	179359.6541	179359.7162(57)	- 22.8	129.127
15 (75, 86) $\rightarrow$ 14 (75, 85)	179359.6541	179359.7162(57)	- 22.8	129.127
15 (76, 87) $\rightarrow$ 14 (76, 86)	179359.6541	179359.7162(57)	- 22.8	129.127
15 (77, 88) $\rightarrow$ 14 (77, 87)	179359.6541	179359.7162(57)	- 22.8	129.127
15 (78, 89) $\rightarrow$ 14 (78, 88)	179359.6541	179359.7162(57)	- 22.8	129.127
15 (79, 90) $\rightarrow$ 14 (79, 89)	179359.6541	179359.7162(57)	- 22.8	129.127
15 (80, 91) $\rightarrow$ 14 (80, 90)	179359.6541	179359.7162(57)	- 22.8	129.127
15 (81, 92) $\rightarrow$ 14 (81, 91)	179359.6541	179359.7162(57)	- 22.8	129.127
15 (82, 93) $\rightarrow$ 14 (82, 92)	179359.6541	179359.7162(57)	- 22.8	129.127
15 (83, 94) $\rightarrow$ 14 (83, 93)	179359.6541	179359.7162(57)	- 22.8	129.127
15 (84, 95) $\rightarrow$ 14 (84, 94)	179359.6541	179359.7162(57)	- 22.8	129.127
15 (85, 96) $\rightarrow$ 14 (85, 95)	179359.6541	179359.7162(57)	- 22.8	129.127
15 (86, 97) $\rightarrow$ 14 (86, 96)	179359.6541	179359.7162(57)	- 22.8	129.127
15 (87, 98) $\rightarrow$ 14 (87, 97)	179359.6541	179359.7162(57)	- 22.8	129.127
15 (88, 99) $\rightarrow$ 14 (88, 98)	179359.6541	179359.7162(57)	- 22.8	129.127
15 (89, 100) $\rightarrow$ 14 (89, 99)	179359.6541	179359.7162(57)	- 22.8	129.127
15 (90, 101) $\rightarrow$ 14 (90, 100)	179359.6541	179359.7162(57)	- 22.8	129.127
15 (91, 102) $\rightarrow$ 14 (91, 101)	179359.6541	179359.7162(57)	- 22.8	129.127
15 (92, 103) $\rightarrow$ 14 (92, 102)	179359.6541	179359.7162(57)	- 22.8	129.127
15 (93, 104) $\rightarrow$ 14 (93, 103)	179359.6541	179359.7162(57)	- 22.8	129.127
15 (94, 105) $\rightarrow$ 14 (94, 104)	179359.6541	179359.7162(57)	- 22.8	129.127
15 (95, 106) $\rightarrow$ 14 (95, 105)	179359.6541	179359.7162(57)	- 22.8	129.127
15 (96, 107) $\rightarrow$ 14 (96, 106)	179359.6541	179359.7162(57)	- 22.8	129.127
15 (97, 108) $\rightarrow$ 14 (97, 107)	179359.6541	179359.7162(57)	- 22.8	129.127
15 (98, 109) $\rightarrow$ 14 (98, 108)	179359.6541	179359.7162(57)	- 22.8	129.127
15 (99, 110) $\rightarrow$ 14 (99, 109)	179359.6541	179359.7162(57)	- 22.8	129.127
15 (100, 111) $\rightarrow$ 14 (100, 110)	179359.6541	179359.7162(57)	- 22.8	129.127
15 (101, 112) $\rightarrow$ 14 (101, 111)	179359.6541	179359.7162(57)	- 22.8	129.127
15 (102, 113) $\rightarrow$ 14 (102, 112)	179359.6541	179359.7162(57)	- 22.8	129.127
15 (103, 114) $\rightarrow$ 14 (103, 113)	179359.6541	179359.7162(57)	- 22.8	129.127
15 (104, 115) $\rightarrow$ 14 (104, 114)	179359.6541	179359.7162(57)	- 22.8	129.127
15 (105, 116) $\rightarrow$ 14 (105, 115)	179359.6541	179359.7162(57)	- 22.8	129.127
15 (106, 117) $\rightarrow$ 14 (106, 116)	179359.6541	179359.7162(57)	- 22.8	129.127
15 (107, 118) $\rightarrow$ 14 (107, 117)	179359.6541	179359.7162(57)	- 22.8	129.127
15 (108, 119) $\rightarrow$ 14 (108, 118)	179359.6541	179359.7162(57)	- 22.8	129.127
15 (109, 120) $\rightarrow$ 14 (109, 119)	179359.6541	179359.7162(57)	- 22.8	129.127
15 (110, 121) $\rightarrow$ 14 (110, 120)	179359.6541	179359.7162(57)	- 22.8	129.127
15 (111, 122) $\rightarrow$ 14 (111, 121)	179359.6541	179359.7162(57)	- 22.8	129.127
15 (112, 123) $\rightarrow$ 14 (112, 122)	179359.6541	179359.7162(57)	- 22.8	129.127
15 (113, 124) $\rightarrow$ 14 (113, 123)	179359.6541	179359.7162(57)	- 22.8	129.127
15 (114, 125) $\rightarrow$ 14 (114, 124)	179359.6541	179359.7162(57)	- 22.8	129.127
15 (115, 126) $\rightarrow$ 14 (115, 125)	179359.6541	179359.7162(57)	- 22.8	129.127
15 (116, 127) $\rightarrow$ 14 (116, 126)	179359.6541	179359.7162(57)	- 22.8	129.127
15 (117, 128) $\rightarrow$ 14 (117, 127)	179359.6541	179359.7162(57)	- 22.8	129.127
15 (118, 129) $\rightarrow$ 14 (118, 128)	179359.6541	179359.7162(57)	- 22.8	129.127
15 (119, 130) $\rightarrow$ 14 (119, 129)	179359.6541	179359.7162(57)	- 22.8	129.127
15 (120, 131) $\rightarrow$ 14 (120, 130)	179359.6541	179359.7162(57)	- 22.8	129.127
15 (121, 132) $\rightarrow$ 14 (121, 131)	179359.6541	179359.7162(57)	- 22.8	129.127
15 (122, 133) $\rightarrow$ 14 (122, 132)	179359.6541	179359.7162(57)	- 22.8	129.127
15 (123, 134) $\rightarrow$ 14 (123, 133)	179359.6541	179359.7162(57)	- 22.8	129.127
15 (124, 135) $\rightarrow$ 14 (124, 134)	179359.6541	179359.7162(57)	- 22.8	129.127
15 (125, 136) $\rightarrow$ 14 (125, 135)	179359.6541	179359.7162(57)	- 22.8	129.127
15 (126, 137) $\rightarrow$ 14 (126, 136)	179359.6541	179359.7162(57)	- 22.8	129.127
15 (127, 138) $\rightarrow$ 14 (127, 137)	179359.6541	179359.7162(57)	- 22.8	129.127
15 (128, 139) $\rightarrow$ 14 (128, 138)	179359.6541	179359.7162(57)	- 22.8	129.127
15 (129, 140) $\rightarrow$ 14 (129, 139)	179359.6541	179359.7162(57)	- 22.8	129.127
15 (130, 141) $\rightarrow$ 14 (130, 140)	179359.6541	179359.7162(57)	- 22.8	129.127
15 (131, 142) $\rightarrow$ 14 (131, 141)	179359.6541	179359.7162(57)	- 22.8	129.127
15 (132, 143) $\rightarrow$ 14 (132, 142)	179359.6541	17935		

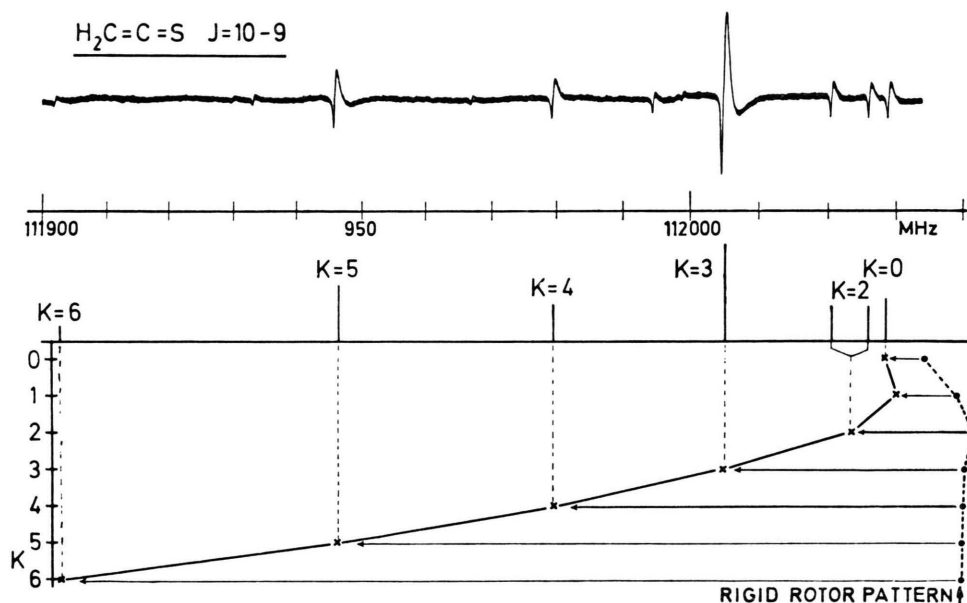


Fig. 2. Observed spectrum of thioketene at 112 GHz with a typical  $K_a$  pattern ( $K_a$  represented by  $K$ ). The center of the  $K_a = 1$  and 2 transitions is indicated in the diagram.

had to be rejected. Several other measured transitions were also rejected from the fit, indicating an error in measurement or overlap with excited state lines. The standard deviation of the least squares analysis was obtained to be 16.5 kHz, which corresponds to the assumed reproducibility of the frequency measurements.

#### IV. Centrifugal Distortion Analysis

The centrifugal distortion analysis of the observed rotational spectrum was performed using Watson's reduced Hamiltonian in the  $I^r$  axis representation [18]. As in previous papers on ketene [3, 4], the A-reduced form of the Hamiltonian operator with  $R_6 = 0$  was used first to calculate the rotational energy levels. Further refinement of the distortion constants could not be achieved with this form. The higher inertial symmetry of thioketene made it necessary to use the S-reduced Hamiltonian according to Watson, in which  $R_5$  is zero. The complete form of this operator with the constants used is given below:

$$\begin{aligned} \mathcal{H} = & \frac{1}{2} (B + C) \hat{P}^2 + [A - (B + C)/2] \hat{P}_z^2 \\ & - D_J \hat{P}^4 - D_{JK} \hat{P}^2 \hat{P}_z^2 - D_K \hat{P}_z^4 + H_{JK} \hat{P}^4 \hat{P}_z^2 \\ & + H_{JK} \hat{P}^2 \hat{P}_z^4 - L_{KJ} \hat{P}^2 \hat{P}_z^6 + S_{KJ} \hat{P}^2 \hat{P}_z^8 \end{aligned}$$

$$\begin{aligned} & + [(B - C)/4 + d_1] \hat{P}^2 \cdot [\hat{P}_+^2 + \hat{P}_-^2] \\ & + d_2 \hat{P}^2 \cdot [\hat{P}_+^4 + \hat{P}_-^4] \end{aligned}$$

with

$$\hat{P}_\pm = \hat{P}_x \pm i \hat{P}_y.$$

$\hat{P}$ ,  $\hat{P}_x$ ,  $\hat{P}_y$ , and  $\hat{P}_z$  are the operators for the total angular momentum and its components. The constants  $A$ ,  $B$  and  $C$  are Watson's reduced rotational constants in the  $I^r$  axis representation. Only two sextic constants have been used in our calculations. In addition to the sextic terms we found it necessary to add two higher order terms,  $L_{KJ}$  and  $S_{KJ}$ , in order to fit the observed transitions with  $K_a$  values of 6 and 7. The reduced spectroscopic constants in the  $I^r$  axis representation are given in Table 2.

As was pointed out by Nemes and Winnewisser [4], a-type rotational spectra of nearly symmetric prolate rotors contain information about the difference  $(A - D_K)$ , but not about  $A$  and  $D_K$  separately. In order to obtain the best possible  $A$  constant the value of  $D_K$  was taken from ketene [3] and was held fixed in the least squares analysis. The uncertainty of  $D_K$  might cause a larger error of  $A$  than that calculated from the least squares analysis and given in Table 2. The remaining rotational constants and the quartic and sextic constants are well determined. The octic constant  $L_{KJ}$  is poorly



Table 2. Spectroscopic parameters of thioketene for Watson's reduced Hamiltonian in the  $I^r$ -axis representation<sup>a</sup>.

$A/\text{MHz}$	286 655 (82)
$B/\text{MHz}$	5 659.47596 (72)
$C/\text{MHz}$	5 544.51269 (75)
$D_J/\text{kHz}$	1.08569 (4)
$D_{JK}/\text{kHz}$	168.269 (77)
$D_K/\text{MHz}$	23.5 (fixed)
$d_1/\text{Hz}$	− 25.46 (68)
$d_2/\text{Hz}$	− 5.21 (35)
$H_{JK}/\text{Hz}$	0.716 (20)
$H_{KJ}/\text{Hz}$	− 408.7 (73)
$L_{KJ}/\text{Hz}$	0.65 (24)
$S_{KJ}/\text{Hz}$	− 0.0533 (24)

<sup>a</sup> The standard deviation of the fit is 16.5 kHz for 125 equally weighted lines. Numbers in parentheses are standard errors.

determined and the dectic constant  $S_{KJ}$  shows that the Hamiltonian is not converging properly. These two constants therefore have to be considered only as fitting parameters to allow the measured frequencies of the  $K_a=6$  and  $K_a=7$  lines to be included in the calculations. In order to complete the distortion analysis, perpendicular rovibrational infrared transitions would have to be included.

## V. Dipole Moment

The electric dipole moment for thioketene was determined from Stark effect measurements of the  $2_{02} \leftarrow 1_{01}$  transition to be 1.01 (3) D. This value places thioketene between the homologues ketene, with  $\mu=1.41$  D [3], and selenoketene with  $\mu=0.90$  D [9].

## VI. Discussion

The reduced spectroscopic constants given in Table 2 can be transformed to the so-called determinable constants,  $\mathfrak{A}$ ,  $\mathfrak{B}$ ,  $\mathfrak{C}$ ,  $T_{aa}$ ,  $T_{bb}$ ,  $T_{cc}$ ,  $T_1$  and  $T_2$ , following the notation of Watson [18] and Yamada and Winnewisser [23]. These constants are invariant to a unitary transformation of the Hamiltonian and they are listed together with the derived inertial moments and the  $\tau$ -defect  $\Delta T_{cc}$  in Table 3. The errors of these parameters are estimated from the standard deviations obtained in the least squares analysis. The small value for the  $\tau$ -defect  $\Delta T_{cc}$  permits the application of any of the various

Table 3. Watson's determinable constants and moments of inertia for thioketene<sup>a</sup>.

$\mathfrak{A}/\text{MHz}$	286 655 (82)
$\mathfrak{B}/\text{MHz}$	5 659.64633 (80)
$\mathfrak{C}/\text{MHz}$	5 544.68316 (83)
$I_a/\mu\text{\AA}^2$ <sup>b</sup>	1.76301 (50)
$I_b/\mu\text{\AA}^2$	89.294625 (12)
$I_c/\mu\text{\AA}^2$	91.146056 (13)
$A/\mu\text{\AA}^2$ <sup>b</sup>	0.08842 (53)
$T_{aa}/\text{MHz}$	− 23.66935 (8)
$T_{bb}/\text{kHz}$	− 1.1470 (25)
$T_{cc}/\text{kHz}$	− 1.0452 (25)
$T_1/\text{kHz}$	− 171.495 (79)
$T_2^*/\text{kHz}$ <sup>c</sup>	− 4.2204 (34)
$\Delta T_{cc}/\text{Hz}$ <sup>d</sup>	2.3 (73) undefined

<sup>a</sup> Numbers in parentheses are estimated errors on the basis of the standard errors of Table 2.

<sup>b</sup>  $A = I_c - I_a - I_b$ . <sup>c</sup>  $T_2^* = T_2/(\mathfrak{A} + \mathfrak{B} + \mathfrak{C})$ .

<sup>d</sup>  $\Delta T_{cc} = T_{cc} - (T_2 - \mathfrak{C} T_1)/(\mathfrak{A} + \mathfrak{B})$ .

planarity relations [23] in order to obtain the complete set of derived quartic distortion constants as was done in the case of ketene [4].

In the discussion of the previous section it was shown that the addition of higher order terms in the Hamiltonian was necessary to fit the  $K_a=6$  and  $K_a=7$  transitions. However, the inclusion of these terms did not prove useful in predicting the line positions of the  $K_a=8$  lines, which could not be found at the expected positions. Though their intensities are rather low, we believe that the Hamiltonian used is insufficient to allow good frequency predictions outside the observed range of  $K_a$  states. No predictions for  $K_a>7$  lines were therefore included in Table 1.

In a recent communication Yamada [24] has explained and analyzed the observed anomaly found in the  $^1R_5$  and  $^1R_6$  branches of the far infrared spectrum of HNCO. An interaction between the  $K_a=6$  and 7 levels in the ground vibrational state and the  $K_a=5$  and 6 levels in the lowest excited vibrational state is caused in HNCO by a centrifugal distortion correction term in the Hamiltonian. Although the  $K_a$  energy levels in the ground vibrational state of  $\text{H}_2\text{CCS}$  are lower in energy ( $A \sim 30 \text{ cm}^{-1}$  for HNCO,  $9.5 \text{ cm}^{-1}$  for  $\text{H}_2\text{CCS}$ ), the ratio of the rotational constant  $A$  to the energy of the lowest bending mode is probably similar for HNCO and  $\text{H}_2\text{CCS}$ . Thus the lowest bending mode of  $\text{H}_2\text{CCS}$  can be expected to be involved in this type

of resonance for some value of  $K_a$ . The symmetry selection rules are analogous in the two cases. The network of Coriolis interactions in HNCN is similar to that in  $\text{H}_2\text{CCO}$  [5, 6] and therefore a corresponding set of interactions can be expected in  $\text{H}_2\text{CCS}$ , favoring an interaction with the ground state.

#### Acknowledgements

The authors would like to express their thanks to Dr. B. M. Landsberg for suggesting this problem and

for his help in the initial stages of this work. We also thank Dr. K. Yamada for his help and discussions concerning the centrifugal distortion analysis, and Dr. B. P. Winnewisser for critically reading and commenting on the manuscript.

This work was supported in part by funds from the Deutsche Forschungsgemeinschaft, the Max-Planck-Institut für Radioastronomie and the Fonds der Chemischen Industrie.

- [1] B. Bak, E. S. Kundsén, E. Madsén, and J. Rastrup-Andersen, *Phys. Rev.* **79**, 190 (1950).
- [2] H. R. Johnson and M. W. P. Strandberg, *J. Chem. Phys.* **20**, 687 (1952).
- [3] J. W. C. Johns, J. M. R. Stone, and G. Winnewisser, *J. Mol. Spectrosc.* **42**, 523 (1972).
- [4] L. Nemes and M. Winnewisser, *Z. Naturforsch.* **31a**, 272 (1976).
- [5] L. Nemes, *J. Mol. Spectrosc.* **72**, 102 (1978).
- [6] P. D. Mallinson and L. Nemes, *J. Mol. Spectrosc.* **59**, 470 (1976).
- [7] K. Georgiou, H. W. Kroto, and B. M. Landsberg, *J. Chem. Soc. London, Chem. Commun.* **1974**, 739.
- [8] B. Bak, O. J. Nielsen, H. Svanholt, A. Holm, N. H. Toubro, A. Krantz, and J. Laureni, *Acta Chem. Scand. A* **33**, 161 (1979).
- [9] B. Bak, O. J. Nielsen, H. Svanholt, and A. Holm, *Chem. Phys. Letters* **53**, 374 (1978).
- [10] B. Bak, O. J. Nielsen, H. Svanholt, and A. Holm, *Chem. Phys. Letters* **55**, 36 (1978).
- [11] B. E. Turner, *Astrophys. J.* **213**, L 75 (1977).
- [12] M. A. Frerking, R. A. Linke, and P. Thaddeus, *Astrophys. J.* **234**, L 143 (1979).
- [13] R. A. Linke, M. A. Frerking, and P. Thaddeus, *Astrophys. J.* **234**, L 139 (1979).
- [14] H. Bock, B. Solouki, G. Bert, and P. Rosmus, *J. Amer. Chem. Soc.* **99**, 1663 (1977).
- [15] O. P. Strausz, R. K. Gosavi, F. Bernardi, P. G. Mercy, J. D. Goddard, and I. G. Scrimadia, *Chem. Phys. Letters* **53**, 211 (1978).
- [16] A. Krantz and J. Laureni, *J. Amer. Chem. Soc.* **96**, 6768 (1974).
- [17] E. Schäfer, Diplom-Arbeit, Justus-Liebig-Universität, Gießen 1978.
- [18] J. K. G. Watson, Aspects of Quartic and Sextic Centrifugal Effects on Rotational Energy Levels, in: *Vibrational Spectra and Structure*, J. R. Durig, Editor; Elsevier, Amsterdam 1977.
- [19] M. Winnewisser, *Z. Angew. Physik* **30**, 359 (1971).
- [20] M. Winnewisser and B. P. Winnewisser, *Z. Naturforsch.* **29a**, 633 (1974).
- [21] D. A. Helms, M. Winnewisser, and G. Winnewisser, *J. Phys. Chem.*, in press 1980.
- [22] C. A. Burrus, *Solid State Electronics* **7**, 219 (1964).
- [23] K. Yamada and M. Winnewisser, *Z. Naturforsch.* **31a**, 131 (1976).
- [24] K. Yamada, *J. Mol. Spectrosc.*, in press 1980.